Available online at www.sciencedirect.com
ScienceDirect
Journal of Solid State Chemistry 181 (2008) 239–244
JOURNAL OF SOLID STATE CHEMISTRY
www.elsevier.com/locate/jssc

Preparation and characterization of three-dimensionally ordered macroporous yttria-stabilized zirconia by aqueous organic gel route

J.P. Zhao[a,*], Y. Li[b], W.H. Xin[a], X. Li[a]

[a]Department of Applied Chemistry, Harbin Institute of Technology, No. 92 Xida zhi Street, Harbin 150001, PR China
[b]Center for Composite Materials, Harbin Institute of Technology, Harbin 150001, PR China

Received 10 September 2007; received in revised form 4 November 2007; accepted 12 November 2007
Available online 17 November 2007

Abstract

Three-dimensionally ordered macroporous (3-DOM) yttria-stabilized zirconia (YSZ) was prepared by aqueous organic gel method through the interstitial spaces between polystyrene spheres assembled on glass substrates. The morphologies and pore size of the porous YSZ were characterized by scanning electron microscope (SEM) and nitrogen adsorption. The thermal behavior, the phase and chemical composition of PS/YSZ composite were investigated by Fourier transform infrared spectroscopy (FT-IR), X-ray diffraction (XRD) and X-ray photoelectron spectroscopy (XPS). The results show that porous YSZ has been formed with the pores arranged in an ordered close-packed three-dimensional structure. Ni/YSZ cermet was also prepared by immersing the 3-DOM YSZ into the solution of nickel nitrate and urea. The electrical conductivity of Ni/YSZ was about 400 $S\,cm^{-1}$ between 600 and 800 °C.

Keywords: Three-dimensionally ordered macroporous (3-DOM); Yttria-stabilized zirconia (YSZ); Aqueous organic gel method; Ni/YSZ; Electrical conductivity

1. Introduction

Porous yttria-stabilized zirconia (YSZ) is becoming increasingly important because of a variety of applications, such as separation media for liquid or gas filtration processes, thermal insulators, sensors and supports for solid oxide fuel cell (SOFCs) [1,2]. According to their applications, the fabrication process must be carefully controlled to obtain sufficient porosity, different pore sizes and microstructure. In the past few years, a new approach using colloidal crystals as self-assembled templates for macropores has been used to prepare macroporous materials with well-defined pore sizes and controlled three-dimensional ordering [3–6]. A typical procedure to prepare three-dimensionally ordered macroporous (3-DOM) materials with colloidal crystals templates includes three steps, i.e. self-assembly of the template, infiltration of the desired precursor and removal of the template. Wet chemistry techniques, such as sol–gel process, have been successfully applied to prepare the precursor of macroporous solid materials [7–12]. However, the major disadvantage of the alkoxide-based sol–gel process is that the alkoxide precursor solution is extremely sensitive to moisture and has to be processed under a strictly dry atmosphere. It becomes more difficult to fill the voids, if the hydrolysis and condensation rates are too rapid. Moreover, the high cost and difficulty of obtaining some commercial metal alkoxides hinder the research progress in the fabrication of 3-DOM materials.

Aqueous organic gel method, based on complex between metal cations and hydroxycarboxylic acid, is an alternative to sol–gel process [13–15]. This method has the advantages of using common reagents, low cost, homogeneous mixing at molecule level, good stoichiometric control, low processing temperature, use of an aqueous based processing system and no need for a special atmosphere. Despite these advantages, to the best of our knowledge, there are no papers that describe the preparation of 3-DOM YSZ materials by using aqueous organic gel method. In this work, YSZ aqueous precursors were first introduced into the spaces between the templating polystyrene (PS) sphere

*Corresponding author. Fax: +86 451 86402345.
E-mail address: jpzhao@hit.edu.cn (J.P. Zhao).

0022-4596/$ - see front matter © 2007 Elsevier Inc. All rights reserved.
doi:10.1016/j.jssc.2007.11.007

arrays and well-ordered macroporous YSZ was prepared. The thermal decomposition of PS/YSZ composite and phase transformation during the calcination process were reported. In addition, Ni/YSZ cermet was prepared and the electrical conductivity was measured.

2. Experimental

2.1. Preparation of macroporous YSZ and Ni/YSZ

The starting materials used were styrene (C_8H_8, 99.99%), potassium persulphate ($K_2S_2O_8$, 99.99%), $ZrOCl_2 \cdot 8H_2O$ (99.99%), $Y(NO_3)_3 \cdot 6H_2O$ (99.99%), $Ni(NO_3)_2 \cdot 6H_2O$ (99%), nitric acid, citric acid, urea and ammonia solution.

Monodisperse PS spheres with an average diameter of 510 ± 10 nm and relative standard deviation smaller than 4% (on the diameter) were obtained by using an emulsifier-free emulsion polymerization technique [16]. Then, aqueous PS latex was centrifuged at 3000 rpm for 5 h and allowed to dry under vacuum to form PS macropore templates.

For the preparation of YSZ precursor, zirconium oxychloride and yttrium nitrate were dissolved in citric acid aqueous solution with the molar ratio of citric acid:metal cations = 1.5:1. The pH was raised to 8 by the addition of ammonia solution. The solution was then evaporated at 80 °C to obtain a viscous YSZ precursor, which can be used to infiltrate into the voids of the templates. The concentration of the precursor was varied by dilution with water and methanol. The addition of methanol can increase the wetting between the precursor and template.

The PS templates were then soaked in the YSZ precursor for 12 h and excess solution was removed by vacuum filtration. The obtained PS/YSZ composites were subsequently dried for 6 h and heated in air up to 700 °C for 4 h at a heating rate of 1 °C/min to remove the PS templates and obtain porous structure of YSZ. Porous YSZ was then immersed in an aqueous solution of Ni nitrate and urea. Heating the solution at 100 °C led to the formation of a precipitate. After calcination at 700 °C, the impregnated YSZ was pressed in the shape of a rectangular bar and sintered at 1350 °C for 6 h to form a NiO/YSZ cermet. The air-sintered samples were then reduced under H_2 and Ar atmosphere at 800 °C to reduce NiO to metallic Ni.

2.2. Characterization

The phase composition of the porous YSZ was analyzed by using X-ray diffraction (XRD) on a Phillips X'Pert diffractometer equipped with Cu$K\alpha$ radiation in the range of $2\theta = 20$–80°. Infrared spectroscopy was used for studying the coordinated structure of PS/YSZ composites. The samples, mixed with 99 wt% KBr, were pressed into pellets for IR examination in the frequency range 350–4000 cm^{-1}. Morphological investigation was performed using a LEO-15 FEG-SEM scanning electron microscope. The samples were sputter-coated with gold before examination. X-ray photoelectron spectroscopy (XPS) analysis was performed on a Perkin-Elmer PHI 5000 C XPS system with a monochromatic Mg$K\alpha$ source and charge neutralizer. All the binding energies were referenced to C 1*s* peak at 284.6 eV of the surface adventitious carbon. The nitrogen adsorption–desorption data were obtained from a Micromeritics ASAP 2010. Electrical conductivity was measured using a four-probe method. Platinum paint was used as a contact for electrical measurements.

3. Results and discussion

3.1. Morphology of porous YSZ

SEM image of the PS/YSZ composite, i.e. after infiltration of YSZ precursor but before template removal is shown in Fig. 1(a). The filling of the YSZ precursor has occurred through all the layers of the template and the ordering of the spheres has been maintained, while there are some cracks which have not been infilled. SEM images of porous YSZ calcined at 600 °C are shown in Fig. 1(b) and (c). Well-ordered hexagonal structures can be observed in the top-view images. A second layer of the network, with the same ordering structure, can also be observed through the first layer (Fig. 1(c)). The hexagonal packing of the PS spheres replicated in the pore arrangement of YSZ. The center-to-center distance between the air spheres is measured as 375 nm, which is about 26.5% smaller than the diameter of PS spheres used to form templates.

Nitrogen adsorption–desorption measurements were performed on 3-DOM YSZ. The isotherm shows monolayer–multilayer adsorption at low pressure and a steep slope at high pressures associated with capillary condensation (Fig. 2). The hysteresis loops between adsorption and desorption modes are associated with capillary condensation in the mesopore structure. This behavior suggests that the porous networks consist of mesopores, which have diameter smaller than that of the main voids. The BET surface area is about 45 m^2/g and the average BJH pore diameter is about 32.5 nm.

3.2. Thermal behavior of PS/YSZ composites

In order to investigate the phase development of PS/YSZ composite with increasing calcination temperature and the interactions between PS templates and YSZ precursor, the composites were dried at 60 °C and calcined at 200–600 °C for 4 h, respectively. The obtained samples were characterized by IR. Figs. 3 and 4 show the IR spectra of pure PS, PS/YSZ composite and the samples calcined at different temperatures. The peaks at 3082, 3059, 3024 cm^{-1} can be assigned to the stretching vibration of C–H in the benzene ring of PS (Fig. 3(a)). The absorption bands at 2920 and 2848 cm^{-1} can be attributed to $-CH_2-$ symmetric and

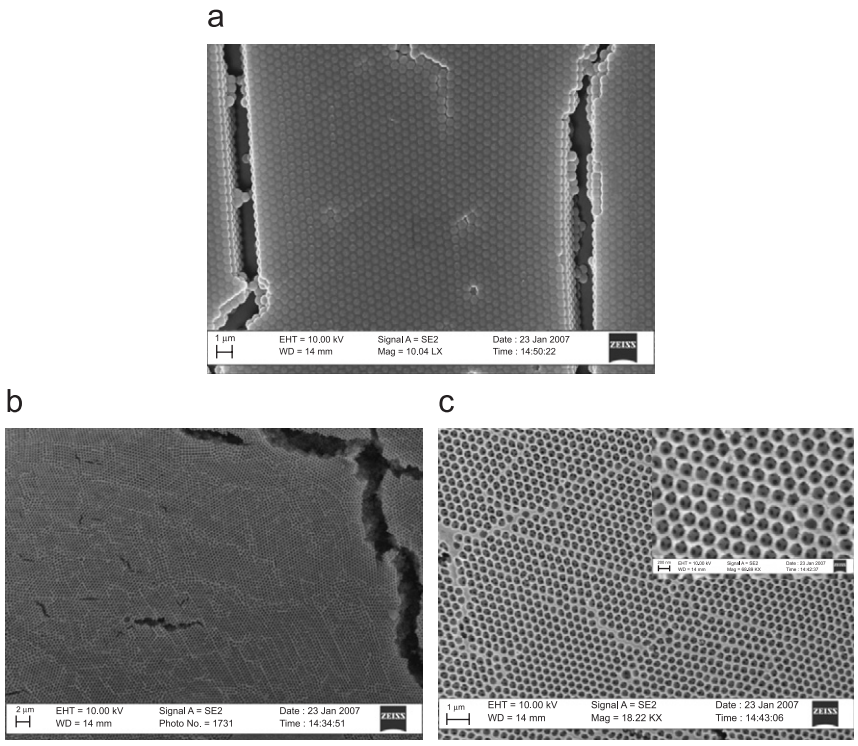

Fig. 1. SEM micrographs showing the surfaces of (a) PS/YSZ composite, (b and c) 3-DOM YSZ structure at different magnifications. The inset in (c) is a magnified top view.

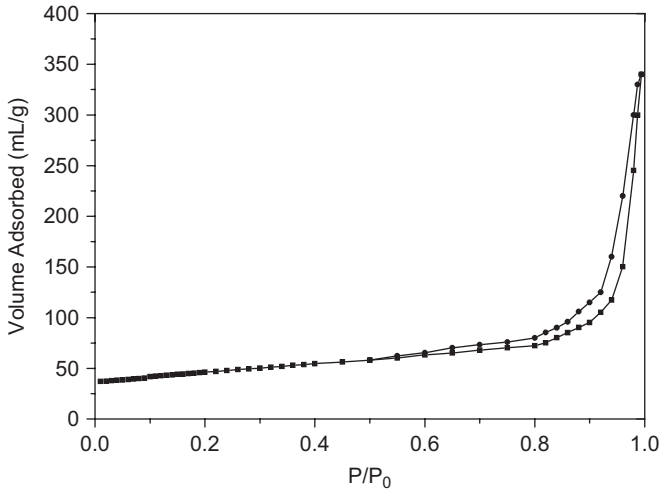

Fig. 2. N_2 adsorption–desorption isotherms of 3-DOM YSZ.

asymmetric stretching vibrations. Three peaks at 1600, 1492 and 1451 cm^{-1} can be attributed to benzene ring vibrations of PS. The bands at 756 and 695 cm^{-1} can be assigned to flexural vibrations of benzene ring.

For the spectrum of PS/YSZ composite dried at 60 °C (Fig. 3(b)), because citric acid is excessive, a significant shoulder at 1730 cm^{-1} is assigned to the $\nu(C=O)$ stretch of citric acid. Moreover, a characteristic band appears at 1393 cm^{-1} corresponding to the symmetric

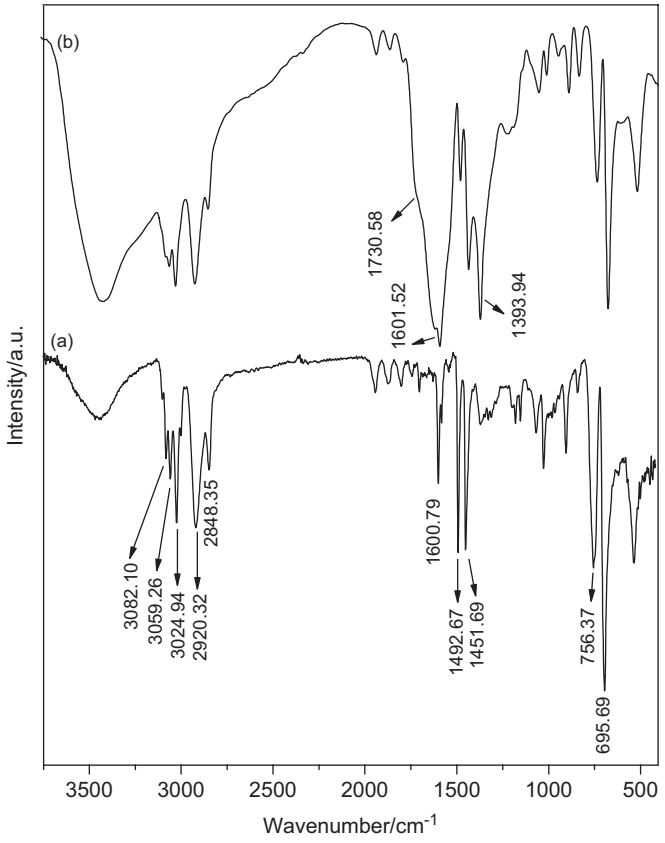

Fig. 3. IR spectra of (a) pure PS and (b) PS/YSZ composite dried at 60 °C.

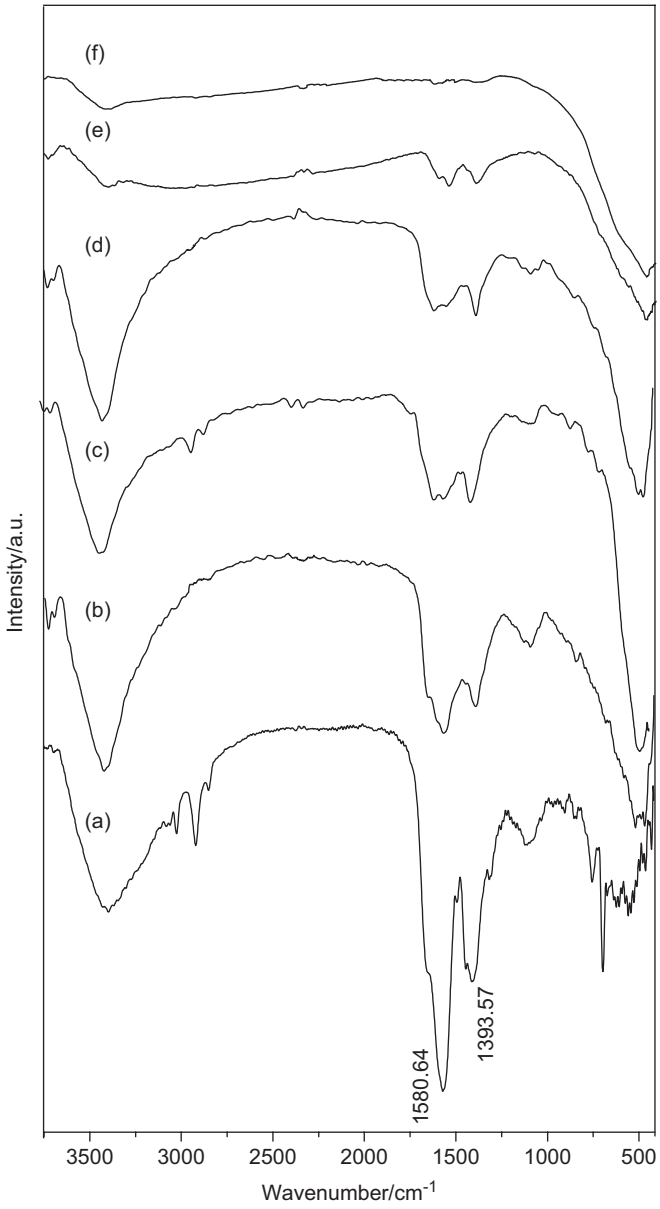

Fig. 4. IR spectra of (a) PS/YSZ composite calcined at 200 °C, (b) YSZ precursor calcined at 200 °C, (c) PS/YSZ composite calcined at 300 °C, (d) YSZ precursor calcined at 300 °C, (e) PS/YSZ composite calcined at 400 °C and (f) PS/YSZ composite calcined at 600 °C.

COO^- stretching vibration in carboxylate group ($v_s(COO^-)$). However, the broad band at 1600 cm^{-1} is probably an overlap of the $v_{as}(COO^-)$ stretching vibration, so it is difficult to determine $v_{as}(COO^-)$ accurately. Meanwhile, the characteristic bands of PS at 3059, 3024, 756 and 695 cm^{-1} are still found.

For a better characterization of the structure of YSZ precursor, the pure YSZ precursor was calcined at 200 and 300 °C, respectively. The IR spectrum of the pure YSZ precursor calcined at 200 °C is shown in Fig. 4(b). The $v(C{=}O)$ stretching band at 1730 cm^{-1} of pure citric acid is absent. Instead, two characteristic bands appear at 1580 and 1393 cm^{-1} corresponding to the symmetric and asymmetric COO^- stretching vibrations in carboxylate group ($v_s(COO^-)$, $v_{as}(COO^-)$). This indicates the coordination of the citric acid to metal cations. From the wavenumber separation, Δ, between $v_{as}(COO^-)$ and $v_s(COO^-)$, the coordination type can be interpreted [17]. The carboxylate group may bind to a metal cation in either a monodentate, bidentate or bridging fashion. As $\Delta \approx 180\ cm^{-1}$, it indicates that bridging coordination forms between Zr^{4+} and the COO^- group of citric acid. In comparison to Fig. 4(b), the major difference between Fig. 4(a) and (b) is that there are characteristic bands of PS in the spectrum of PS/YSZ composite (Fig. 4(a)). The bands at 1580 and 1393 cm^{-1} corresponding to $v_s(COO^-)$, $v_{as}(COO^-)$ can also be observed. These findings would suggest that citric acid has coordinated to metal ions to form a complex, while chemical interactions do not occur between the YSZ precursor and PS spheres in the PS/YSZ composite.

In the spectrum of the composite calcined at 300 °C (Fig. 4(c)), small characteristic bands of PS at 2920 and 2848 cm^{-1} still remain, indicating that PS is not completely removed at this temperature. The absorption bands at 1580 and 1393 cm^{-1} related to a COO^- stretching mode remain in the spectrum of the sample, but the intensity of the stretching is reduced. This demonstrates that at this temperature a partial decomposition of the organic components is occurring. At 400 °C (Fig. 4(e)), vibrations at about 520 cm^{-1} associated with metal oxygen stretching are observed, which indicates the presence of YSZ phase. Vibration bands relative to PS disappear, evidencing the complete removal of the organic template by this process. On further heating to 600 °C (Fig. 4(f)), the bands of organic compounds disappear and the band of Zr–O stretching vibration at 520 cm^{-1} becomes prominent.

Fig. 5 shows the XRD patterns of the PS/YSZ composite calcined in air at 300, 400, 600 and 700 °C for 4 h, respectively. The results indicate that the precursor is amorphous when heat-treated at and below 300 °C. Precursors heat-treated at 600 °C can form the desirable phase. With rise in the temperature of heat treatment, the degree of crystallinity of YSZ increases. The porous samples are polycrystalline with cubic YSZ phase, which has been formed directly from the thermal decomposition of the precursors without passing through any intermediate phases.

The samples calcined at 400 and 600 °C were investigated by XPS. In Fig. 6, the XPS survey spectra of porous YSZ are shown. According to the result, the sample contains only Zr, Y, O as well as a small amount of carbon. The binding energies of the peaks associated with Zr, Y and O are the same for both the spectra, while the peak intensity increases with the temperature. The existence of C 1*s* peak is mainly caused by CO_2, which is absorbed by the surface of the sample.

In Fig. 7(a)–(c), detailed high-resolution spectra of Zr 3*d*, Y 3*d* and O 1*s* core levels at 45° takeoff angles are shown. The position of the Zr $3d_{3/2}$ peak in ZrO_2 is found at

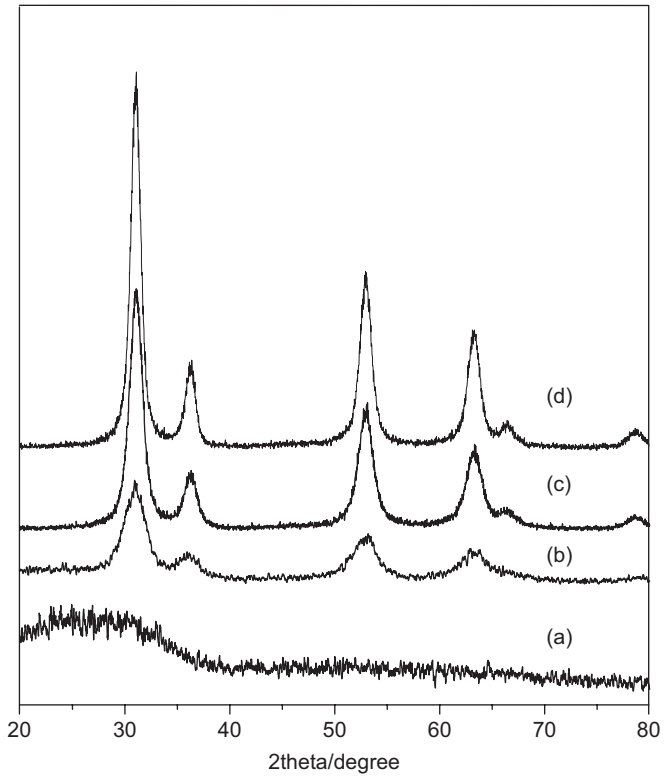

Fig. 5. X-ray diffractograms of porous YSZ calcined at (a) 300 °C, (b) 400 °C, (c) 600 °C and (d) 700 °C for 4 h in ambient air.

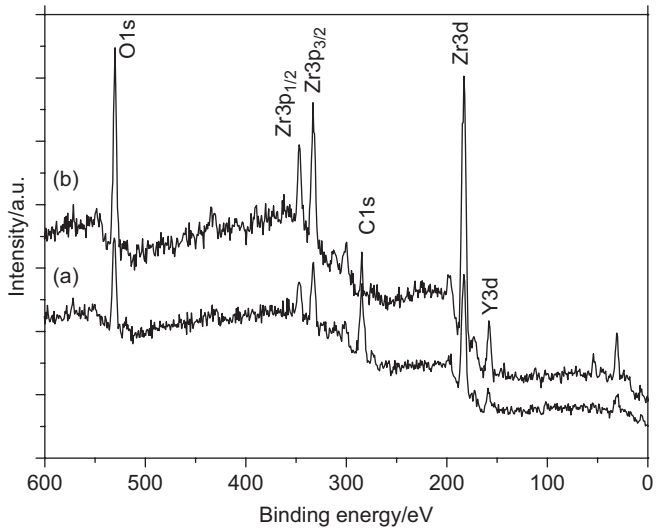

Fig. 6. Survey XPS spectra of 3-DOM YSZ calcined at (a) 400 °C and (b) 600 °C.

184.4 eV. The Y $3d_{3/2}$ peak appears at a binding energy of 158.8 eV (E_b for pure Y_2O_3 is 158.4 eV). The binding energies of Zr 3*d* and Y 3*d* peaks indicate that the samples consist of Y_2O_3 and ZrO_2. There is no clear change for the XPS spectra of O 1*s* energy levels at 400 °C (not shown) and 600 °C (Fig. 7(c)). The oxygen 1*s* signal can be resolved into two peaks, where the main peak at a binding energy of 529.4 eV refers to the lattice oxygen of YSZ and a smaller

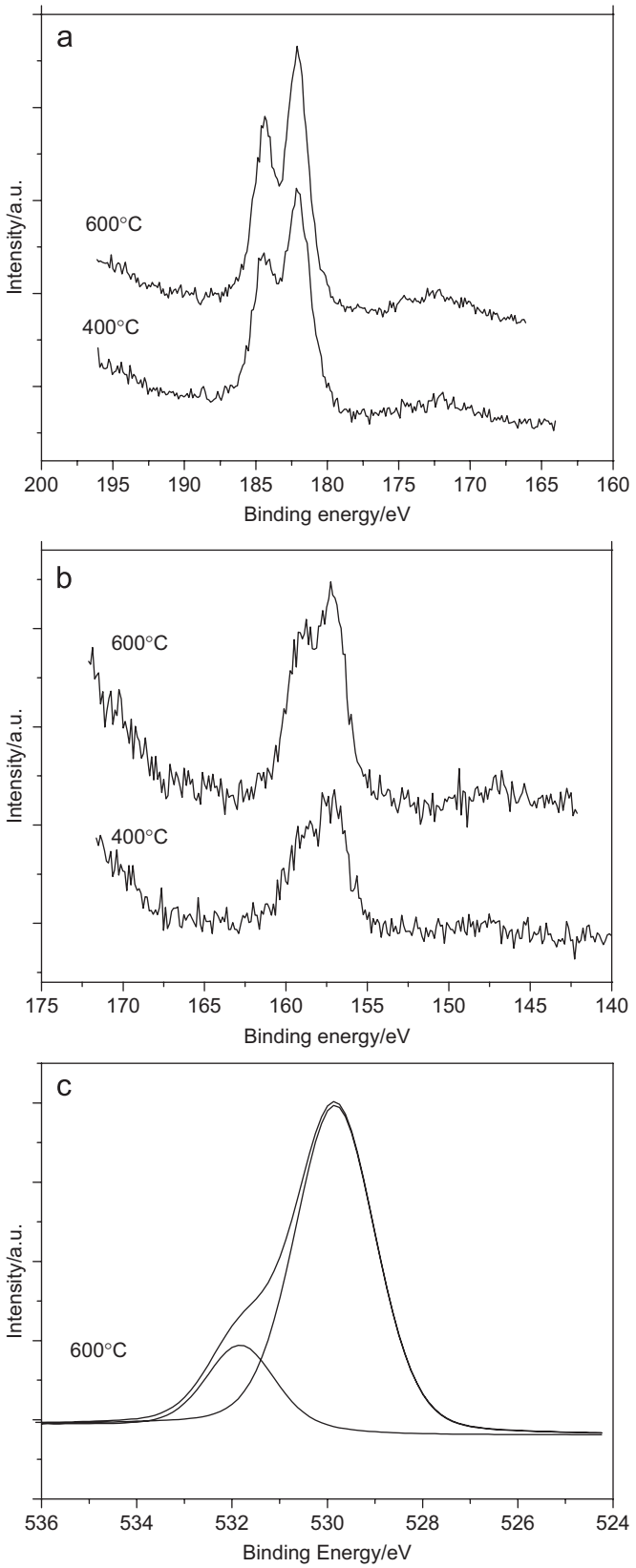

Fig. 7. XPS spectra of (a) Zr 3*d* doublet, (b) Y 3*d* doublet and (c) O 1*s* in 3-DOM YSZ calcined at 400 and 600 °C.

Table 1
XPS composition results for 3-DOM YSZ calcined at 400 and 600 °C

	Sample (at%)			
	Zr	Y	O	C
400 °C	10.8	2.3	48.9	38.0
600 °C	15.2	3.3	60.3	21.2

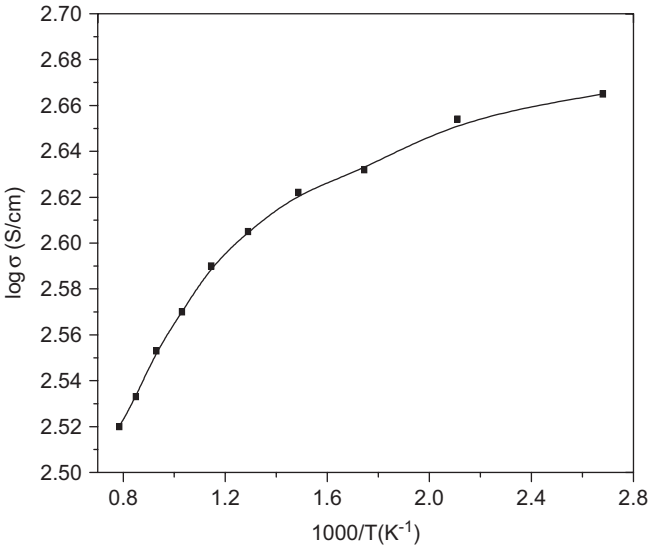

Fig. 8. The relation between electrical conductivity and temperature of Ni/YSZ cermet.

one at 531.8 eV can be ascribed to adsorbed oxygen. In Table 1, the concentrations of elements determined from the XPS spectra at different temperatures are listed as atomic ratios. It is clearly seen that the concentrations of oxygen, zirconium and yttrium increase by increasing temperature. This suggests that the YSZ organic precursor completely decomposes into oxides at elevated temperature.

3.3. Electrical conductivity of Ni/YSZ

The electrical conductivity is shown in Fig. 8 as a function of reciprocal of the temperature. It shows a nonlinear relationship between $\log\sigma$ and $1/T$, which indicates that the ionic conductance exists resulting from the continuous network of YSZ. The electrical conductivity decreases with increasing temperature, demonstrating the electronically conductive characteristics of a metal. The conductivity is about $400\,S\,cm^{-1}$ between 600 and 800 °C, which is an intermediate value compared with that of Ni/YSZ cermet prepared by the other methods [18,19]. Further research should be done to find the optimal processing parameter that will increase the Ni/YSZ conductivity.

4. Conclusions

Ordered macroporous YSZ is achieved by filling PS templates with YSZ aqueous organic precursor via a transformation process. Nitrogen adsorption–desorption measurements show that the porous networks consist of mesopores having diameters smaller than those of the main voids. The results of FT-IR, XRD and XPS have confirmed that in the YSZ precursor, citric acid has coordinated to metal ions to form a complex. No chemical interactions occur between the YSZ precursors and PS spheres in PS/YSZ composite. The desirable cubic phase has formed after calcination at 600 °C. The oxidation level of YSZ is verified by XPS and the binding energies are in agreement with Y_2O_3 and ZrO_2. Ni/YSZ cermet was also prepared and the electrical conductivity was about $400\,S\,cm^{-1}$ between 600 and 800 °C. Further research should be done to find the optimal processing parameter that will increase the Ni/YSZ conductivity.

Acknowledgments

This work was supported by the National Natural Science Foundation of China (No. 20601006), Natural Science Foundation of Hei Longjiang Province and Program for New Century Excellent Talents in University (NCET2006). The first author acknowledges Prof. J.A. Kilner, Prof. D.W. McComb, Dr. S. Skinner, Dr. M.A. McLachlan and Dr. R. Zhu, Department of Materials, Imperial College London, for discussions and technical assistance.

References

[1] A.J. Burgraaf, Fundamentals of Inorganic Membrane Science and Technology, Membrane Science and Technology, series 4. Elsevier Science B.V., Amsterdam, 1996, p. 14.
[2] S. de Souza, S.J. Visco, L.C. de Jonghe, Solid State Ionics 98 (1997) 57–60.
[3] A. Imhof, D.J. Pine, Nature 389 (1997) 948–951.
[4] O.D. Velev, T.A. Jede, R.F. Lobo, A.M. Lenhoff, Nature 389 (1997) 447–448.
[5] B.T. Holland, C.F. Blanford, A. Stein, Science 281 (1998) 538–540.
[6] J.E.G.J. Wijnhoven, W.L. Vos, Science 281 (1998) 802.
[7] B. Li, J. Zhou, Q. Li, L.T. Li, Z.L. Gui, J. Am. Ceram. Soc. 86 (2003) 867–869.
[8] C. Verissimo, O.L. Alves, J. Am. Ceram. Soc. 89 (2006) 2226–2231.
[9] Y. Jin, Y.H. Zhu, X.L. Yang, C.Z. Li, J.H. Zhou, J. Solid State Chem. 180 (2007) 300–305.
[10] Y.N. Fu, Z.G. Jin, Z.F. Liu, W. Li, J. Eur. Ceram. Soc. 27 (2007) 2223–2228.
[11] Z.Z. Gu, A. Fujishima, O. Sato, Appl. Phys. A 74 (2002) 127–129.
[12] B.T. Holland, C.F. Blanford, T. Do, A. Stein, Chem. Mater. 11 (1999) 795–805.
[13] Y. Li, J.P. Zhao, B. Wang, Mater. Res. Bull. 39 (2004) 365–374.
[14] R.N. Das, P. Pramanik, Mater. Lett. 46 (2000) 7–14.
[15] T. Asai, E.R. Camargo, M. Kakihana, M. Osada, J. Alloys Compd. 309 (2000) 113–117.
[16] J.H. Kim, M. Chainey, M.S. El-Aasser, J.W. Vanderhoff, J. Polym. Sci. A: Polym. Chem. 27 (1989) 3187–3199.
[17] K. Nakamoto, Infrared and Raman spectra of Inorganic and Coordination Compounds, Wiley, New York, 1997, p. 65.
[18] M. Mamak, N. Coombs, G. Ozin, Adv. Funct. Mater. 11 (2001) 59–63.
[19] S.K. Pratihar, A. Dassharma, H.S. Maiti, Mater. Res. Bull. 40 (2005) 1936–1944.